Three-Dimensional Analysis of a Rotating Wind Turbine Airfoil

Mohamed Mehdi OUESLATI[1], Anouar Wajdi DAHMOUNI[1], Sassi Ben NASRALLAH[2]

[1]Laboratory of Wind Energy Management and Waste Energy Recovery, Research and Technologies Center of Energy Ecoparck of Borj-Cedria , BP 95 Hammam lif 2050, Tunisia

[2]Laboratory of Thermal and Energy Systems Studies , National Engineering School of Monastir, Street Ibn El Jazzar, Monastir 5000, Tunisia

*Email: **mehdi.oueslati@crten.rnrt.tn**, dahmouni_anouar_wajdi@yahoo.fr, sassi.bennasrallah@enim.rnu.tn*

Abstract : The wind turbines efficiency, depends on the aerodynamic performances of the airfoil constituting the rotor blades. However, these performances are influenced by the unsteady behavior of the wind (speed and direction) as well as the centrifugal force due to the rotational motion. For that, in this paper a three-dimensional simulation of the flow around a horizontal axis wind turbine model was performed using the Fluent software, to study the characteristics of the flow around a rotating airfoil. The k-ε turbulence model and the Moving Reference Frame (MRF) technique have been used, to take into account the flow turbulence and the rotating effects on the airfoil. The obtained results show that the flow characteristics of the rotating airfoil depend on the tip speed ratio of the wind turbine, the airfoil angle of attack and its radial position along the blade.

Keywords : Three dimensional simulation, rotating airfoil, horizontal axis wind turbine

1. Introduction

To evaluate wind turbine performances it's necessary to examine the flow over the rotor, and take into account the different physical phenomena that can be present during the system operation. Experimentally, the control of the different physical parameters is very difficult and expensive, for that, many researchers were used the fully three-dimensional simulations of wind turbines in complete geometry.

Johansen *et al.* [1] have developed a CFD solver, EllipSys3D, with a stationary RANS model to evaluate the three-dimensional aerodynamic coefficients in different radial positions along the blade. The obtained results were injected into a Blade Element Momentum (BEM) code without additional corrections. They showed excellent compatibility with experimental results for cases when the flow is attached and when small separation flow occurs. Chaviaropoulos *et al.* [2] have solved the Navier Stokes equations in three-dimensional formulation to determine the aerodynamic coefficients under three-dimensional effects. They have remarked that the lift and drag coefficients increase compared with the two-dimensional coefficients and they can be expressed in terms of the chord length, the radius of the rotor and of the local angle of attack. Carangiu *et al.* [3] have developed a three-dimensional CFD model to analyze the influence of the radial flow on the performances of a horizontal axis wind turbine in the range of Reynolds numbers greater than10^6. They have examined the behavior of the boundary layer over the wind turbine blades and they confirmed the increase of the aerodynamic coefficients, however, their results have not been validated experimentally.

Shen *et al.* [4] have developed an analytical method to determine the relative angle of attack of the airfoil and its aerodynamic coefficients at each blade section of a horizontal axis wind turbine based on a three-dimensional CFD results which are validated experimentally. The simulations were carried out in full geometry case of "Tellus" wind turbine which has 95 kW of power using the EllipSys3D solver with a fully turbulent RANS model. By assuming that the transition effects are very limited in the case of the large rotor, they have confirmed the occurrence of the phenomenon of the dynamic stall and the increase of forces acting on the blades by the rotation effect. Yu *et al.* [5] have performed three-dimensional CFD calculations using RANS equations and k-ω SST turbulence model of the NREL horizontal axis wind turbine Phase VI, operating under transition

flow conditions. They showed a good agreement with the existent experimental results for wind speed lower than 10 m/s. Under these conditions, they extrapolated the lift and drag coefficients at angles of attack up to 20°.

Herráez *et al.* [6] have recently modeled the rotor of the horizontal axis wind turbine of the MEXICO project using the three-dimensional CFD solver, OpenFoam, coupled with the single-Spalart Allmaras turbulence model. Their model has been validated by plotting the distribution of the pressure coefficient Cp in comparison with experimental results obtained by PIV measurements. They have confirmed the presence of the dynamic stall phenomenon and the increase of the lift coefficient due to the rotation of the blade. They have attributed the phenomenon of dynamic stall to the Coriolis force effects and the increase of the lift coefficient to the centrifugal force.

Since the studies of the flow characteristics on a rotating wind turbine blades are limited, in this paper three-dimensional simulations of the flow over a horizontal axis wind turbine model have been performed using the Fluent software, to study the influence of the tip speed ratio on the blade performances in different radial positions.

2. Methodology

2.1. Description of the wind turbine model

The horizontal axis wind turbine model studied here had a three bladed rotor. The geometric characteristics are summarized in Table 1.

Tableau 1 : Titre tableau

Parameters	Scale (mm)
Rotor diameter	376
Hub diameter	60
Nacelle length	205
Length of the blade	150
Constant chord length	50

The geometry of the turbine presented in Fig. 1 allows us to study its performances at low tip speed ratio for fixed pitch angle equal to 14.5°. The blades were built from wood which can reproduce accurately the NACA 4412 airfoil geometry (Figure 2). The constant nature of the airfoil along the blades and the constant chord length were chosen to minimize the parameters that can affect the blade performances and highlight the influence of the tip speed ratio dependent only from the rotation speed.
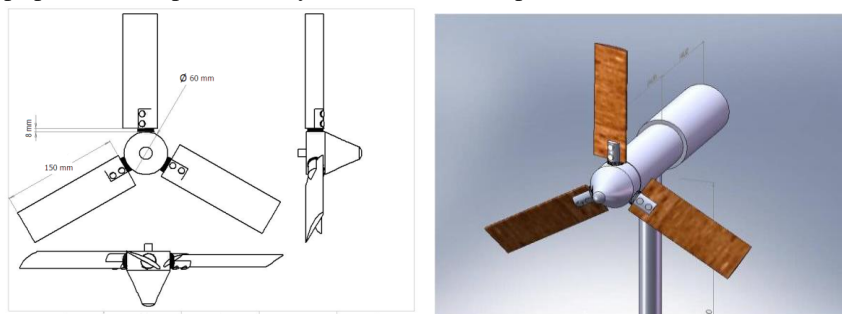
Figure 1 : The three-dimensional design of the horizontal axis wind turbine model
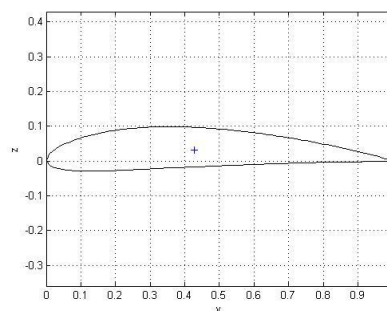
Figure 2 : Airfoil shape of NACA4412**.**

2.2. Grid Generation and Boundary Conditions

The three dimensional unsteady simulations of the wind turbine model operating in a channel were performed using Fluent software package V.6.3.26 and the Gambit software to mesh the domain. The configuration considered is shown in Figure 3.
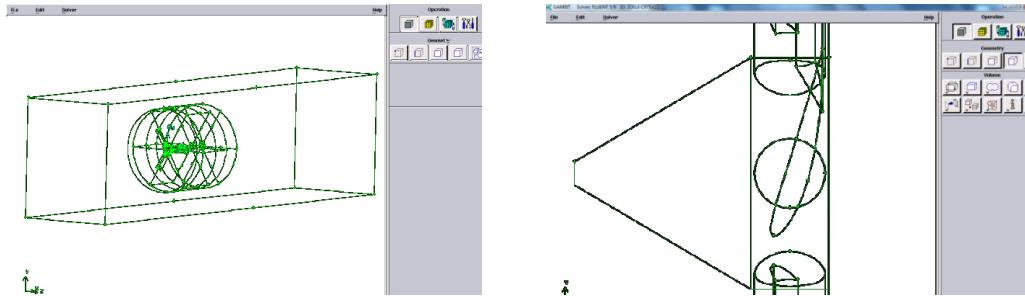
Figure 1 Wind turbine rotor in the plane (x,y)

The unsteady simulations need the division of the computational domain into two sub-domains to ensure the rotation of the rotor. The first zone is a rectangular fixed outer region and the second is an inner rotating zone containing the rotor and the nacelle body in which the near wake will be explored.

The faces in contact with each other between the two regions ensure the continuity of the fluid flow and the relative motion of the inner zone. Concerning the geometric model of the wind turbines only the support tower has been neglected because as mentioned by Gebhardt *et al.* [7] the presence of the turbine support tower does not change the aerodynamic performances of the rotor and also to minimize the complexity of the geometry which reduce the cell numbers.

The mesh block technique was used to optimize the distribution of the cells in the studied geometry. The mesh was tetrahedral around the rotor and into the channel and it was hexahedral in the near wake region behind the rotor. The total mesh was consists of 3,324,776 cells. The grid refinement was focused in the near wake downstream of the wind turbine at the positions of the tip and root vortices as well as around the blades in the radial direction. The Figure 4, shows the refinement downstream of the turbine and around a blade section.
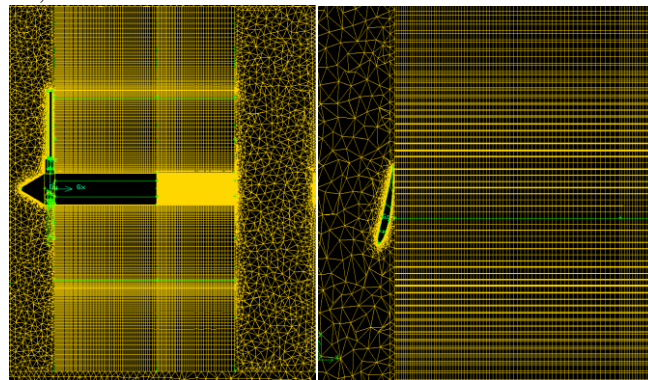
Figure 4 : mesh refinement behind the rotor

The model was placed at a distance of 8×R from the inlet and the boundary condition associated to the upstream velocity was "velocity inlet". The boundary conditions designated to the channel outlet and the channel walls were "pressure outlet" and "stationary wall" respectively as shown in figure 5.
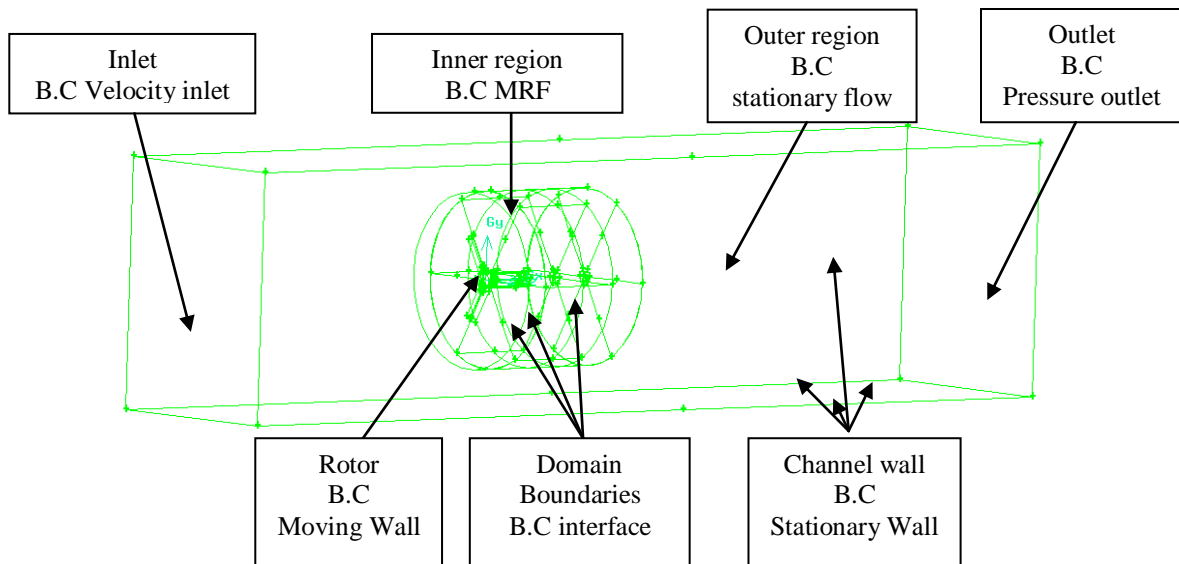
Figure 5 : Boundary conditions

The turbine rotor was associated to "Moving Wall" boundary condition and the flow field around the rotor and the near wake region as a "Moving Reference Frame (MRF)". And finally the turbine nacelle was associated to "Stationary Wall".

The mobile reference system technique in Fluent (MRF: Moving Reference Frame) was used in the simulations to model problems involving moving parts activating mobile referential systems in selected areas. When this option is enabled, the equations of motion are modified to incorporate the terms of Coriolis acceleration occurring due to the transformation of a fixed reference system to a moving reference system. The second order upwind scheme was used for the spatial discretization of the density, the momentum and the turbulent viscosity equations.

2.3. The turbulence Model

During the simulations three turbulence models have been tested: The Standard k-ε model, the RNG k-ε model and the k-ω SST model. The RNG k-ε model has the less accuracy of the results in comparison with the experiments however the Standard k-ε model and the k-ω SST model have the best results accuracy but the Standard k-ε model has more sensitivity to y+ study for that it has been chosen during this simulations.

3. Results and Discussions

The numerical results were validated with experimental results obtained by Dahmouni [8]. He has performed experimental investigations over the wind turbine model described previously placed in the CRTEn wind tunnel using the Particle Image Velocimetry (PIV) technique to study the wind turbine near wake characteristics as shown in Fig. 6.
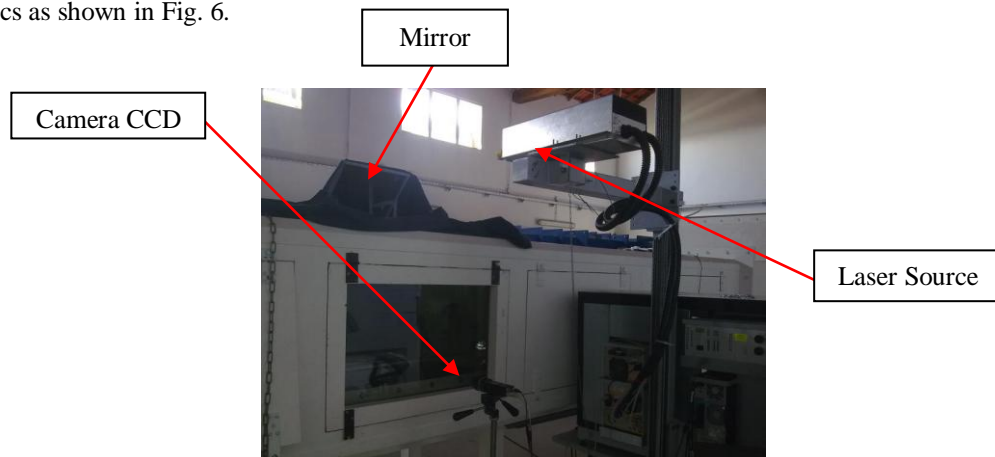
Figure 6 : La soufflerie équipée par le système PIV

To validate the numerical results we have choose the case of tip speed ratio equal to $\lambda = \dfrac{\omega R}{U_\infty} = 4.08$.

During the simulations, the tip speed ratio of the wind turbine λ = 4.08 corresponding to 8.03 m/s of the flow velocity at the inlet of the channel.

Figure 7 illustrates the results from CFD calculations. The iso-surfaces of the axial velocity in the near wake of the wind turbine were presented. It is observed that the near wake downstream is characterized by the detachment of the tip and root vortices from the blades. The helical nature of the vortex shedding was also observed.
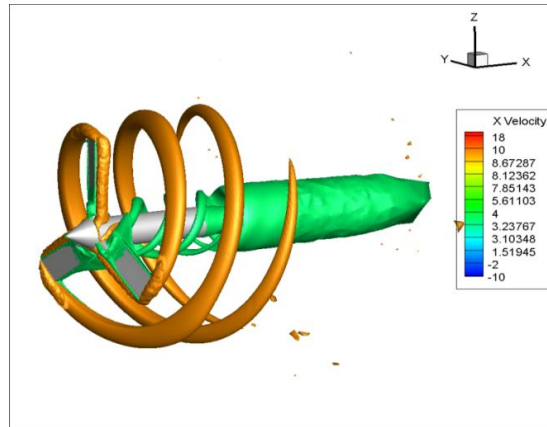
Figure 7 : Three dimensional iso-surfaces of axial velocity for λ=4.08

The qualitative comparison between the numerical and experimental results of the axial velocity in the near wake of the wind turbine is illustrated in Figure 8.
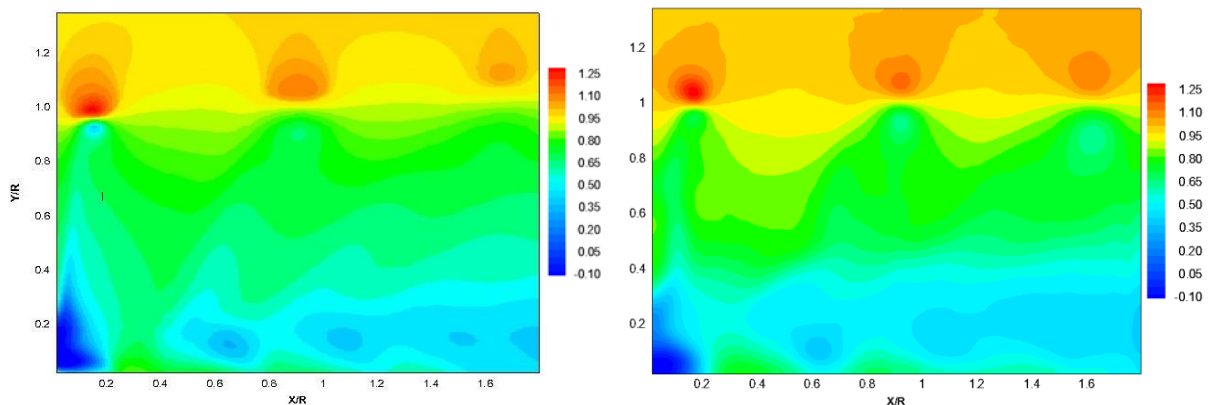
Figure 8 : Axial velocity in the near wake of the wind turbine model : a- numerical results, b-experimental results [8]

The results show a good agreement between numerical and experimental results in the near wake downstream of the wind turbine.

The wake of the wind turbine is generated by the detachment of a helical sheet from the blade and characterized by the presence of two marginal eddies detached from the tip and root of the blades as described above. To more understand the complexity of the wake structure generated, it is necessary to study the flow separation characteristics in each section of the blade in variation with the tip speed of the wind turbine.

This study will be initiated by determining the angle of attack seen by the airfoil at each section of the blade. For this purpose, three different sections in the radial direction were chosen such that: r / R = 0.5, 0.7 and 0.9 where R is the radius of the rotor and r is the position of the airfoil on the blade along the axis Oz as shown in Figure 9.
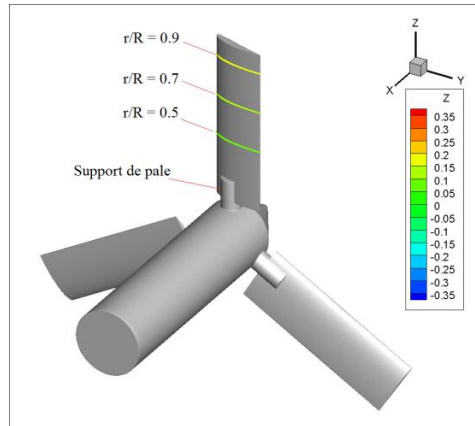
Figure 9 : Airfoil positions in the radial direction of the blade

The attack angle at each blade section can be calculated using the BEM method. It is determined as following:

$$\alpha = \phi - \beta \quad (1)$$

Where ϕ the flow angle, and β is is the pitch angle.

Figure 10 illustrates the geometric parameters and the velocity triangle around a wind turbine blade section.
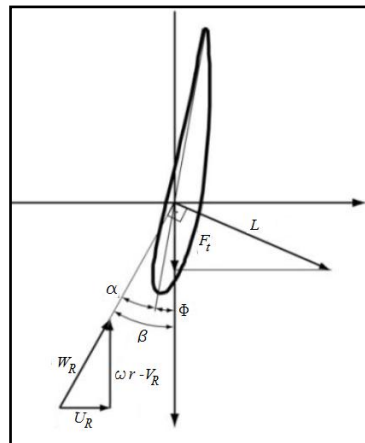
Figure 10 : Geometric parameters of blade section

The flow angle is calculated as follow:

$$\phi = \arctan\left(\frac{U_R}{V_R - \omega r}\right) \qquad (2)$$

The U_R and V_R are the mean axial and tangential velocities in non perturbed flow upstream of the airfoil. By knowing the velocities U_R and V_R, it is possible to determine the flow angle ϕ using the equation (2). Since the pitch angle β is known equal to 14.5°, then the attack angle α can be calculated using equation (1). The results of the variation of the attack angle function of the tip speed ratio at each blade section are shown in Figure 11.
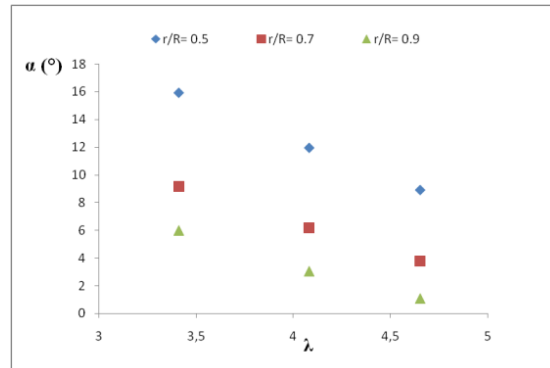
Figure 11 : Variation of the attack angle with tip speed ratio at different positions along the blade r/R=0.5, 0.7 et 0.9

We can clearly show that the attack angle decreases with the increase of the tip speed ratio λ and with the approaching to the blade tip.

3.1. Study of the flow around the airfoil at the radial position r/R = 0.5

Figure 12 shows the axial velocity field around the airfoil at the radial position on the blade equal to r/R=0.5 for different tip speed ratios λ = 3.41, 4.08 and 4.65 corresponding to a rotational speed equal to 1391 rpm, 1664 rpm and 1897 rpm respectively for a constant upstream wind speed equal to 8.03 m/s.

a- 0.5R λ= 3.41

b- 0.5R λ= 4.08

c- 0.5R λ= 4.65
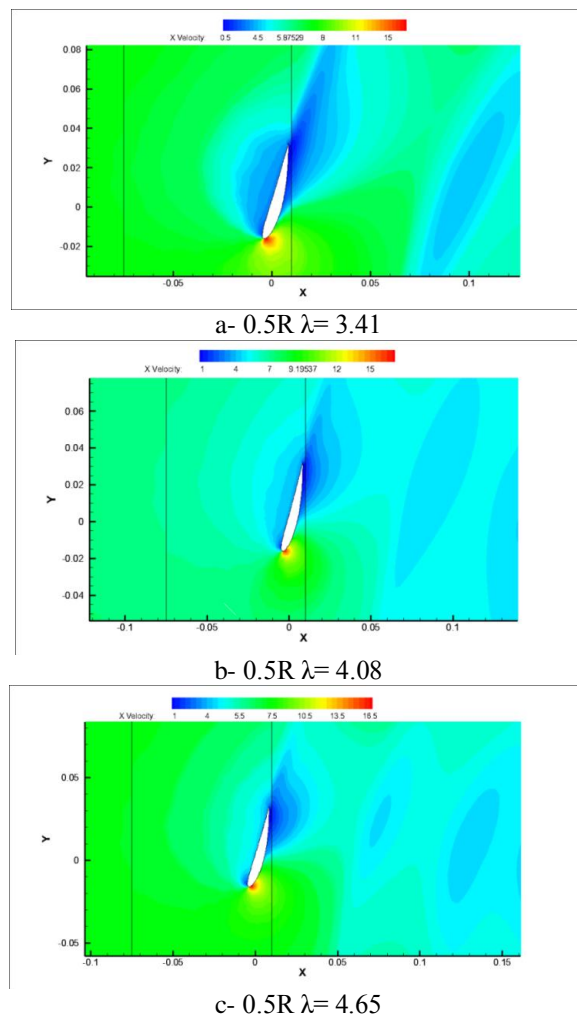
Figure 12 : Axial velocity around the airfoil at the radial section r/R = 0.5 and different tip speed ratios equal to λ= 3.41, 4.08 et 4.65 respectively

Indeed, for the rotation speed of 1391 rpm, a separation zone is observed on the upper surface of the airfoil from 30% of the chord. As the tip speed ratio increases, the attack angle seen by the airfoil decreases as shown in Figure 11, and the separation point moves towards the trailing edge about 50% of the chord length.

3.2. Study of the flow around the airfoil at the radial position r/R = 0.7

Figure 13 shows the axial velocity field for the flow around the airfoil at the blade section r/R=0.7. It is found that the separation point is around 60% of the chord length and moves gradually towards the trailing edge as a function of the increase in the rotational speed of the wind turbine.

a-   0.7R λ= 3.41

b-   0.7R λ= 4.08
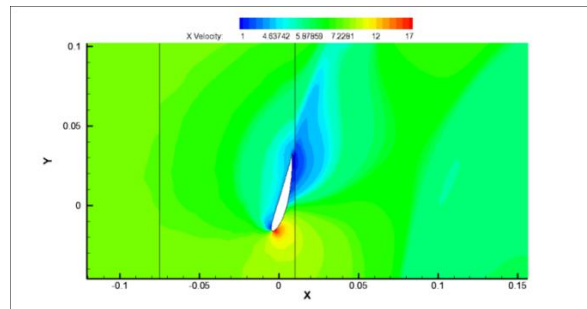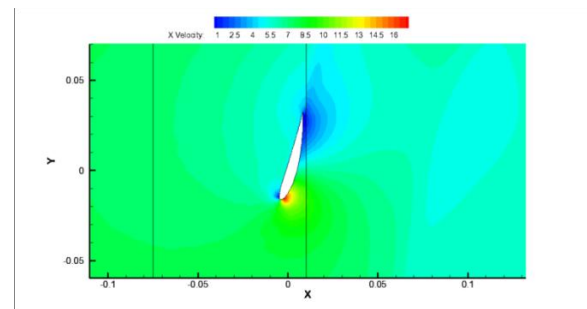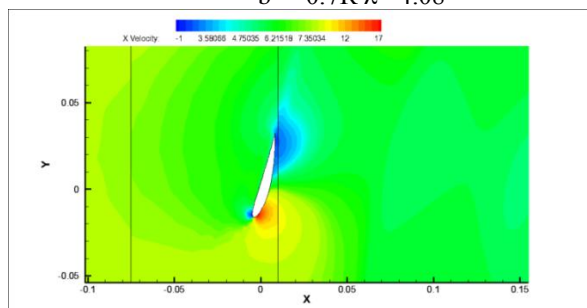
c-   0.7R λ= 4.65

Figure 13 : Axial velocity around the airfoil at the radial section r/R = 0.7 and different tip speed ratios equal to λ= 3.41, 4.08 et 4.65 respectively

3.3. Study of the flow around the airfoil at the radial position r/R = 0.9

Figure 14 shows the axial velocity field around the airfoil at the blade section equal to r/R = 0.9. The separation zone gradually decreases by increasing the rotation speed and disappears completely at a tip speed ratio λ = 4.65 because the angle of incidence seen by the airfoil decreases to 1.1°.

a- 0.9R λ= 3.41

b- 0.9R λ= 4.08

c- 0.9R λ= 4.65
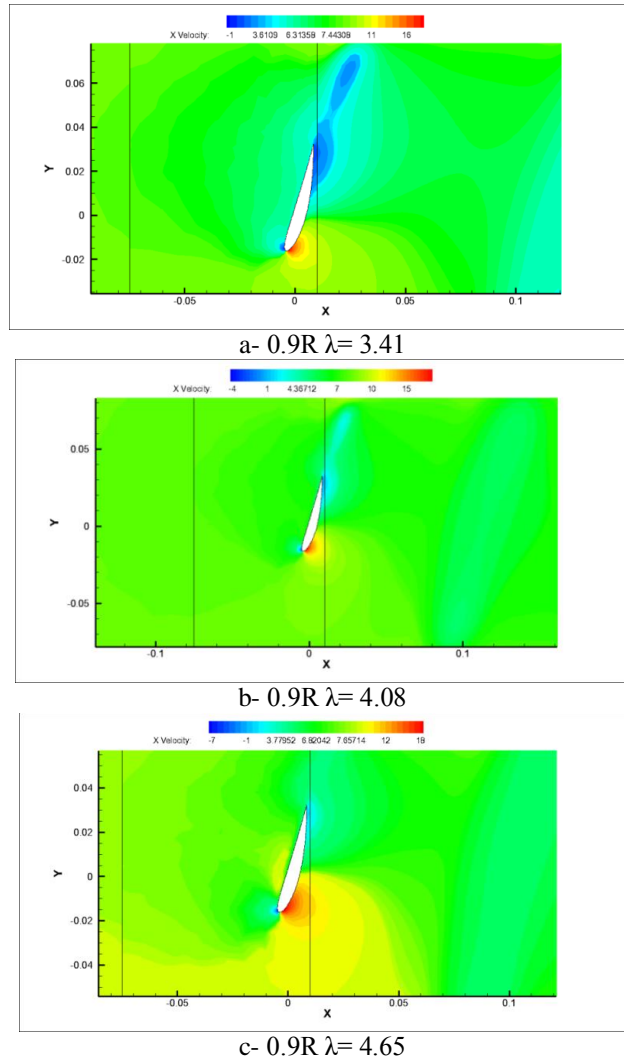
Figure 14 : Axial velocity around the airfoil at the radial section r/R = 0.9 and different tip speed ratios equal to λ= 3.41, 4.08 et 4.65 respectively

3.4. Vorticity field around the rotating airfoil at different positions

Figure 15 shows the vorticity field around the airfoil for the different blade sections r / R = 0.5, 0.7, and 0.9 respectively for λ = 4.08.
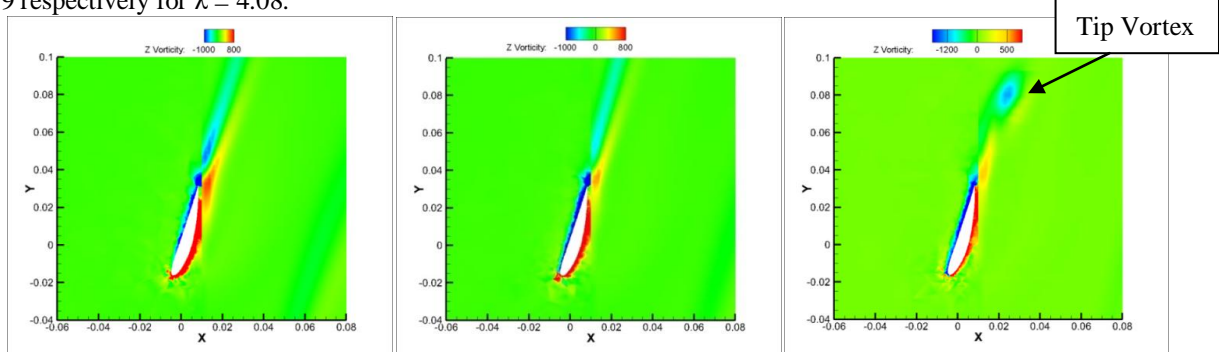
Figure 15 : Vorticity field around the blade sections 0.5R, 0.7R, and 0.9R respectively for tip speed ratio λ=4.08

The detachment of the vortex structures is observed from the trailing edge of the airfoil at each blade sections. In the case where r/R = 0.9, the plane projection of the tip vortex detached from the blade tip is observed.

Conclusion

In this paper a three dimensional analysis of the performances of a horizontal axis wind turbine has been performed. Three- dimensional simulations coupled by the k-ε turbulence model using the Fluent software has been investigated.

The flow characteristics around a rotating wind turbine airfoil at different radial sections have been studied in function of the tip speed ratio. The results show that the attack angle decreases when the tip speed ratio increases which influence the detachment mechanism of the flow in the radial direction along the rotating blade. The rotational speed of the wind turbine influence the centrifugal force acting on the blade which affects it's performances at the leading edge at each blade section in the radial direction.

Nomenclature

Symbole   Nom, *unité*

R	Rotor Radius, *m*		
r	Radial position, *m*		
U_∞	Velocity inlet, *m/s*		
U_R	Axial velocity, *m/s*		
V_R	Tangential velocity, *m/s*		

Symboles grecs

α	Attack angle, °
β	Pitch angle, °
ϕ	Flow angle, °

Références

[1] J. Johansen and N. N. Sørensen, Aerofoil Characteristics from 3D CFD Rotor Computations, *Wind Energy*, Volume 7, Pages 283-294, 2004.

[2] P. K. Chaviaropoulos and M. O. L. Hansen, Investigating Three-Dimensional and Rotational Effects on Wind Turbine Blades by Means of a Quasi-3D Navier Stokes Solver, *Journal of Fluids Engineering*, Volume 122, Pages 330-336, 2000.

[3] C. E. Carcangiu, J. N. Sørensen, F. Cambuli and N. Mandas, CFD–RANS analysis of the rotational effects on the boundary layer of wind turbine blades, *Journal of Physics: Conference Series*, Volume 75, 2007.

[4] W. Z. Shen, M. O. L. Hansen and J. N. Sørensen, Determination of the Angle of Attack on Rotor Blades, *Wind Energy*, Volume 12, Pages 91-98, 2009.

[5] G. Yu, X. Shen, X. Zhu and Z. Du, An insight into the separate flow and stall delay for HAWT, *Renewable Energy*, Volume 36, Pages 69-76, 2011.

[6] I. Herráez, B. Stoevesandt and J. Peinke, Insight into Rotational Effects on a Wind Turbine Blade Using Navier–Stokes Computations, *Energies*, Volume 7, Pages 6798-6822, 2014.

[7] C.G. Gebhardt, S. Preidikman and J.C. Massaa, Numerical simulations of the aerodynamic behavior of large horizontal-axis wind turbines, *International Journal of Hydrogen Energy*, Volume 35, Issue 11,Pages 6005-6011, 2010.

[8] A. W. Dahmouni, Contribution à l'étude des éoliennes, *Thèse de Doctorat*, Ecole National d'ingénieur de Monastir, 2016.